

Yosemite Hydroclimate Network: Distributed Stream and Atmospheric Data for the Tuolumne River Watershed and Surroundings

Jessica D. Lundquist¹, Jim Roche², Harrison Forrester², Courtney Moore³, Eric Keenan¹, Gwyn Perry¹, Nicoleta Cristea¹, Brian Henn¹, Karl Lapo¹, Bruce McGurk⁴, Daniel R. Cayan⁵, and Michael Dettinger⁶

¹Department of Civil and Environmental Engineering, University of Washington, Seattle, WA

²National Park Service, Yosemite, CA

³Northwest Hydraulic Consultants, Seattle, WA

⁴McGurk Hydrologic, Orinda, CA

⁵Scripps Institution of Oceanography, La Jolla, California

⁶United States Geological Survey, Reno, Nevada

15

16

17

18

Corresponding author:

Jessica Lundquist

21 Department of Civil and Environmental Engineering

22 University of Washington

23 201 More Hall, Box 352700

24 Seattle, WA 98195, USA

Email:

26 jdlund@u.washington.edu

28 **Key Points**

29

- 30 • Half-hourly discharge and water temperature data are described and provided for
31 2002-2015 in 8 subbasins of the Tuolumne River, CA.
32 • Daily natural flows are described and provided for the inflow of the Tuolumne River
33 to the Hetch Hetchy Reservoir for 1970 to 2015.
34 • Meteorological data are provided.

35 **Index Terms**

36

37 Streamflow, temperature, hydroclimatology

38

39 **Research Significance**

40

41 This dataset provides a unique opportunity to understand spatial patterns and scaling of
42 hydroclimatic processes in complex terrain and can be used to evaluate downscaling
43 techniques or distributed modeling.

44

45 **Abstract**

46

47 Regions of complex topography and remote wilderness terrain have spatially-varying
48 patterns of temperature and streamflow, but due to inherent difficulties of access, are often
49 very poorly sampled. Here we present a dataset of distributed stream stage, streamflow,
50 stream temperature, barometric pressure, air temperature, and relative humidity from the
51 Tuolumne River Watershed in Yosemite National Park, Sierra Nevada, California, U.S.A. for
52 water years 2002 to 2015, as well as a quality-controlled meteorological forcing time series
53 for use in hydrologic modeling. This paper describes data collected using low-visibility
54 and low-impact installations for wilderness locations and can be used alone or as a critical
55 supplement to ancillary datasets collected by cooperating agencies, referenced herein. This
56 dataset provides a unique opportunity to understand spatial patterns and scaling of
57 hydroclimatic processes in complex terrain and can be used to evaluate downscaling
58 techniques or distributed modeling. The paper also provides an example methodology and
59 lessons learned in conducting hydroclimatic monitoring in remote wilderness.

60

61 **1. Introduction**

62 Mountains are the water towers of the world, with high elevations and complex topography
63 in often protected, wilderness locations. These regions are critical to understand
64 scientifically and yet challenging to observe and monitor. Here we provide a set of
65 distributed measurements of streamflow, water temperature, air temperature, and relative
66 humidity spanning a period of over 10 years in the Tuolumne River Watershed, Yosemite
67 National Park, Sierra Nevada, California, U.S.A. These data could be used for distributed
68 hydrologic modeling, for evaluation of remote sensing products, for testing atmospheric
69 downscaling techniques. Lessons learned from the Tuolumne network can hopefully
70 provide an example of how to establish a similar network in another mountain location.

71 *a. Basin Overview*

72 The upper Tuolumne River Watershed was made famous by John Muir's "first summer
73 in the Sierra" in 1870 (Muir 1911) and became protected as part of Yosemite National Park
74 in 1890. The summer headquarters of the Sierra Club from 1912 to 1973 were located in
75 Tuolumne Meadows beside the river (O'Neill 1984), and the watershed drains to the Hetch
76 Hetchy Reservoir behind the O'Shaughnessy Dam, which was initially constructed in 1923,
77 completed in 1934, and provides hydropower and drinking water to the city of San
78 Francisco and other cities on the San Francisco peninsula. The study area encompasses
79 more high elevations (focus area from 2600-4000 m) and covers a larger total area (over
80 1000 km²) than most research basins in the western U.S. (e.g., Reynolds Creek (Reba et al.
81 2011); the Southern Sierra Critical Zone Observatory (Hartsough and Meadows 2012);
82 Kings River Experimental Watersheds (Hunsaker et al. 2012); Senator Beck (Landry et al.
83 2014)). The location provides both opportunities and challenges. The Tioga Road

84 (California Highway 120), the highest pass over the Sierra Nevada at over 3000 m, provides
85 road access during the summer months only, and many wilderness sites are accessible only
86 by foot. The natural granitic bedrock of the region provides well-controlled, stable stream
87 channels in many locations. The wilderness setting preserves the natural characteristics of
88 the drainage but also requires unique installation practices in order to comply with
89 wilderness regulations, which are detailed further below.

90 The Tuolumne River drainage is fairly typical of the central to southern Sierra Nevada,
91 with its high and cold drainages, winter-precipitation-dominated climate, steep terrain,
92 rapid snowmelt seasons, and relatively thin soils. The area contributing to the Tuolumne
93 River as it enters Tuolumne Meadows is about 186 km², and the area contributing to Hetch
94 Hetchy Reservoir is about 1181 km² (Figure 1). The Tioga glaciation (about 10,000-60,000
95 years ago) removed most sedimentary material, leaving broad U-shaped valleys, polished
96 domes, and steep headwater cirques (Huber 1987). Today two relatively small glaciers,
97 Lyell and Maclure, contribute to the Lyell Fork of the Tuolumne and remain as remnants
98 from the Little Ice Age about 2500 years ago (Basagic and Fountain 2011). Approximately
99 90% of the drainage is underlain by intrusive rocks (chiefly granodiorite; National Park
100 Service (NPS) records of test well drilling), which erode slowly and interact little with the
101 streamflow (Huber, 1987). The underlying granodiorite bedrock in the basin allows us to
102 assume minimal losses to the deep groundwater system, which is a major source of
103 uncertainty in hydrologic observations and modeling in many other locations. The highest
104 third of the Dana Fork sub-basin is underlain by metavolcanic and metasedimentary rock,
105 which tends to be more highly fractured than granodiorite and may result in more
106 subsurface flow than other basin areas. Soil depths are typically 1 m or less, with

107 maximum recorded depths of 3 to 5 in flat meadow locations (Lowry et al. 2011), which is
108 consistent with reported values (Natural Resources Conservation Service, 2006).
109 Precipitation falls primarily as snow (>90% snow for the watershed above the Tuolumne
110 River at Highway 120 in most years), with normal annual peak stream discharge typically
111 occurring in May or June due to snowmelt. Approximately 50% of the drainage area above
112 the Tuolumne River at Highway 120 lies between 2800 and 3300 m elevation, with 25%
113 above and 25% below this range. The dataset here includes stream stage, water
114 temperature and discharge at half-hourly timesteps for water years 2002 to 2015 from a
115 number of sub-basins contributing to this watershed, as well as point and distributed
116 meteorological data (Figure 1; Table 1). We also include daily inflows calculated from the
117 water balance at Hetch Hetchy Reservoir.

118

119 *b. History of the Yosemite Hydroclimate Monitoring Network and unique research
120 results to date*

121 In summer 2001, a group of researchers from Scripps Institution of Oceanography
122 decided to be “high-altitude oceanographers” and began installing pressure transducers in
123 the area’s streams and temperature sensors in the area’s trees. The goal was three-fold – to
124 better understand fine-scale variation in hydroclimatic variables at high elevations
125 (Lundquist et al. 2003), to understand how diurnal cycles in streamflow varied through a
126 watershed system (Lundquist 2004; Lundquist et al. 2005), and to explore the extent to
127 which deployment of numerous, new and inexpensive monitoring instruments—in tandem
128 with a few traditional high-quality measurement stations -- might support greater overall
129 hydrometeorological data coverage in a complex terrain (Bales et al. 2006). Gauge

130 locations were chosen to sample basins with varying elevation ranges, slopes, and aspects,
131 while also considering practicalities, such as access. The most distant site from the road
132 (Lyell Fork below Maclure) samples the basin headwaters immediately downstream of two
133 glaciers, which are a critical source of water in late summer.

134 With the exception of sites adjacent to the road, the entire study area is in federally
135 designated wilderness, where any instrument installations must comply with the
136 Wilderness Act of 1964 (Public Law 88-577) and the National Environmental Policy Act
137 (NEPA) of 1970 (Public Law 91-190). These laws require that installations have the
138 minimum possible impact to the environment, including minimal visibility to wilderness
139 visitors. For this reason, weirs, which are typical in other research catchments, were not
140 used. Instead, installations were designed to be nearly invisible to park visitors desiring a
141 wilderness experience, while still meeting research and operational needs for high data
142 quality, such as providing the Park with essential information for management of floods,
143 water withdrawals, and long-term change (Lundquist and Roche 2009). All sites were
144 developed in close partnership between university researchers, the United States
145 Geological Survey (USGS), and the National Park Service (NPS).

146 Initial years of stream stage data revealed patterns in the timing of how water
147 travels through a snow-fed mountain system. Sometimes a rapid temperature increase
148 causes the onset of spring melt to occur simultaneously across all elevations (Lundquist et
149 al. 2004), although when a similar increase occurs earlier in the year, melt is delayed in
150 north-facing basins because the sun is lower in the sky (Lundquist and Flint 2006). Diurnal
151 cycles in streamflow occur in all of these basins, but the hourly timing of peak flow is
152 controlled by different processes in basins of different sizes (Lundquist and Dettinger

153 2005; Lundquist et al. 2005). Initial years of air temperature data demonstrated how
154 mountain temperatures often do not vary linearly with elevation but still have
155 topographically-predictable spatial patterns (Lundquist and Cayan 2007; Lundquist et al.
156 2008). Similarly, patterns of relative humidity (dewpoint temperature) are more complex
157 than those typically represented in empirical equations based on elevation, but can be
158 captured well by high-resolution atmospheric models (Feld et al. 2013). As years went on,
159 rating curves were developed, and estimated discharge values were used as boundary
160 conditions for simulations of groundwater levels in Tuolumne Meadows (Lowry et al. 2010,
161 2011) and for hydrologic model evaluation (Cristea et al. 2013; Hinkelman et al. 2015) and
162 precipitation evaluation (Henn et al. 2015).

163 The stream network led to new real-time monitoring sites within the basin (Fig. 1).
164 Beginning in water year 2007, the City and County of San Francisco Public Utilities
165 sponsored installation of an official USGS streamflow gaging station in the Tuolumne River
166 just above its inflow to the Hetch Hetchy Reservoir (measuring stage, discharge, water
167 temperature, turbidity and conductivity, and accessible in real-time as USGS gage
168 #11274790 at waterdata.usgs.gov). Fall Creek, which drains to the Hetch Hetchy
169 Reservoir from the north, has historic USGS discharge data (water years 1916 to 1983,
170 USGS gage #11275000) and was reinitialized in 2009 as the FHH site in the
171 cdec.water.ca.gov data system. More recently (in water year 2014), another real-time
172 station, corresponding to the Tuolumne River at Highway 120 site provided here, was
173 established with stage measurements and discharge estimates available at the TUM site in
174 the cdec.water.ca.gov data system.

175 Due to its high elevation and greater-than-average extent of meadows, the
176 Tuolumne River basin has also been a focus of many snow remote sensing studies,
177 including evaluations of snow cover extent (Rice et al. 2011; Raleigh et al. 2013) and snow
178 water equivalent reconstruction (Rittger et al. 2011; [Bair et al. submitted](#)). From water
179 years 2013 to present, the watershed has been a focus of the NASA Airborne Snow
180 Observatory Campaign to use LiDAR to map snow depth at high resolution to aid in
181 forecasting inflow to the Hetch Hetchy Reservoir ([Painter et al. submitted](#)) and was
182 included in pilot flights of the HyspIRI suite of instruments
183 (<http://hyspiri.jpl.nasa.gov/airborne>).

184

185 *c. Outline of this paper*

186 Here we describe an archived and publicly-available dataset for 7 stream locations, 1
187 reservoir, and 62 meteorological locations in the vicinity of the upper Tuolumne River
188 Watershed. Section 2 details the measurement methods and quality control applied, and
189 section 3 describes the basins and their streamflow characteristics. Section 4 offers
190 conclusions and describes applications.

191

192 **2. Datasets**

193 *a. Flow into Hetch Hetchy Reservoir*

194 Full natural flows into the Hetch Hetchy Reservoir were determined on a daily basis
195 through careful consideration of recorded reservoir releases and water levels for water
196 years 1970 to 2015. The uncertainties associated with reconstructed flows are considered
197 to be similar to those of standard streamflow observations ($\sim\pm10\%$).

198

199 *b. Stream stage*

200 Aside from the reservoir, the basis for each record is a pressure transducer anchored to the
201 bottom of the stream channel by either a concrete form or a wilderness stilling tube (see
202 supplemental material here and/or in Lundquist et al. 2009). Data processing included the
203 following: 1) remove data from times when instruments were not in the water; 2) link
204 timeseries data measured by different instruments at the same location (most instruments
205 were swapped with a new self-recording instrument each summer); 3) subtract barometric
206 pressure to obtain a timeseries of water level; 4) use manual stage measurements to adjust
207 the water level timeseries to correct for instrument relocation or drift; and 5) flag or
208 remove obviously erroneous measurements due to ice jams and/or instrument
209 malfunction. The stage obtained from anchored pressure transducers is less reliable than
210 that for stilling tubes because these anchors were sometimes moved by the river at high
211 flow and by field personnel when instruments were replaced. Care was taken to correct for
212 these movements by adding appropriate offsets to the original timeseries, but depending
213 on the availability of manual observations for quality control checks, some errors may
214 remain. The supplemental material ("Overview of the Tuolumne River Streamgauging Sites
215 and Data Processing (pdf)") and site metadata files included with the dataset detail when
216 and where this may be an issue.

217 During recent years, some sites were monitored with a vented pressure transducer
218 in a stilling tube. These pressure sensors have a tube exposing them to atmospheric
219 pressure as well as total stream pressure and do not require separate processing to remove
220 atmospheric pressure, leading to smaller observational uncertainty. Table 2 details the

221 various instruments and installation types, and quantifies expected measurement
222 uncertainties. Although the early measurement system (a pressure sensor in a concrete
223 anchor) were the easiest to install and had the minimal visual impact to the park
224 wilderness, the improved data accuracy from the stilling tube and vented pressure
225 transducer systems more than compensates for the extra installation footprint and effort
226 (~2% error in discharge from this method compared to ~15% error, see Table 2).

227

228 *c. Stream Discharge*

229 Manual discharge observations were taken during the months of May through September
230 each year. Most measurements were made by wading with an AA or pygmy meter
231 (following methods of Rantz et al. 1982a), although acoustic doppler sonar (Oberg and
232 Mueller 2007), dye-dilution (Rantz et al. 1982b, Ch 7), and salt-dilution (Moore 2004a,
233 2004b, 2005; Hudson and Fraser 2005) methods were also used at high flows.
234 Methodologies were tested by taking repeat measurements within the same hour at the
235 same location. During these tests, measurements fell within 5-10% of each other, which
236 can be considered the accuracy of an individual manual discharge measurement reported
237 here.

238 Rating curves were developed to relate stage to discharge for each stream, and best
239 estimates of 95% confidence intervals are provided. Where channel geometry information
240 was available, we combined hydraulic information with stage and discharge measurements
241 following the methodology of LeCoz et al. (2014). This method begins by using the
242 hydraulics of the study site to determine a range of meaningful values for the unknowns in
243 the equation

$$Q=a(h-b)^c \quad (1)$$

For example, the Manning-Stickler equation ($c \sim 1.67$) can be applied to steady-state, uniform flows in a rectangular channel, and the rectangular weir equation ($c \sim 1.5$) can be applied at low flows with a downstream section control. Thus, site surveys and hydraulics were used to create a first guess (Bayesian priors) for the rating curve, and then the manual discharge measurements, with their associated uncertainty (10%), were used in a Bayesian Markov-chain monte-carlo framework to update those rating curves to determine the best fit curve and the associated 95% uncertainty (see details in LeCoz et al. 2014 and in the supplemental material). The methodology was used to determine the best-fit break point between water levels where the rating curve became subject to a downstream section control, and different equations were used for discharge within the two ranges. In cases where water entered the flood plain at high flows, a third equation was added (see supplemental material). Rating curves and associated uncertainty from this methodology were compared with a single rating curve equation and confidence bounds determined by a log-transform least-squares fit to the manual stage-discharge observations (see supplemental material). The best fit curve for the two methodologies was very similar at all stations, but the 95%-confidence intervals for the least-squares methodology were, in general, much tighter at low flows and wider at high flows than the corresponding 95%-confidence intervals determined from the Bayesian methodology. We report the Bayesian confidence intervals in the dataset because they more realistically represent low-flow uncertainty, which is critical to represent fairly since low flows are important to many park management decisions (e.g., when the campground or lodge would need to be closed).

266 Due to the seasonal timing of manual measurements, which were taken between
267 May and September, we are most confident of the calculated streamflow values during the
268 summer (Moore et al. 2014). Both higher and lower flows are associated with lower
269 confidence. Users are advised that due to the limited access and lack of control structures,
270 uncertainties are larger than one would expect at a typical USGS gauge station (see
271 discussion of errors associated with shorter-term gauges in Birgand et al. 2013), but the
272 95% confidence intervals are provided to help indicate this uncertainty. All site surveys
273 and manual measurements are provided so that users may examine and/or recalculate the
274 rating curves or conduct additional uncertainty analysis (e.g., Coxon et al. 2015).

275

276 *d. Barometric pressure*

277 Because most of the stream instruments record absolute pressure, which is the weight of
278 both the water and the atmosphere above them, barometric pressure records were used to
279 remove the effects of atmospheric pressure fluctuations. One timeseries was created using
280 local barometric pressure recorded by Solinst Barologgers and by Hobo Water Level
281 Loggers at a variety of locations (see supplemental material and metadata), because
282 atmospheric pressure was close to spatially uniform over this domain. Pressure
283 transducers are sensitive to instrument temperature fluctuations, and this is not always
284 well-compensated for in instrument software (Freeman et al. 2004). Therefore, care was
285 taken to cross-compare instrument records at times when multiple records were available
286 and to select the instrument subjected to the minimum diurnal air temperature
287 fluctuations at any given time. When possible, this was an instrument in a dry
288 groundwater well because temperature oscillations were muted by the overlying soil. The

289 temperatures recorded by each instrument are provided in case users would like to
290 develop their own further temperature compensation algorithms.

291

292 *e. Standard meteorological forcing data*

293 Hourly temperature, relative humidity, incoming shortwave irradiance, and wind speed
294 data for water years 2003 to 2015 were derived from data collected at the California
295 Department of Water Resources (CA DWR) snow pillow site at Dana Meadows (Figure 1
296 and see supplemental material). Shortwave irradiance was corrected for snow
297 accumulating on the radiometer dome following the methodology of Lapo et al. 2015.

298 Short data gaps (< 2 days in length) were filled with shortwave interpolation (see
299 acknowledgements for link to code), while longer gaps were filled by estimating shortwave
300 according to the MTCLIM methods detailed in (Bohn et al. 2013). Daily accumulated
301 precipitation was measured with a weighing gage at the Tuolumne Meadows snow pillow
302 site. Based on the Parameter Regression against Independent Slopes Model (PRISM; Daly
303 et al. 2008), Dana Meadows (Figure 1) typically received 1.3 times the amount of
304 precipitation as Tuolumne Meadows, and this ratio was verified by comparing snow
305 accumulation rates at the two sites (Cristea et al. 2013). In order to provide meteorological
306 forcing representative of a single site, as is required for many hydrologic models, the Dana
307 precipitation was estimated using this multiplier. Daily precipitation was assumed to occur
308 uniformly over all hours of the day. Years when a tree was growing in the middle of the
309 Dana Meadows snow pillow were excluded from the snow water equivalent data series
310 (Lundquist et al. 2015). Longwave irradiance was not measured. However, an estimate of

311 incoming longwave is provided, using the Prata (1996) and Deardorff (1978) algorithms, as
312 recommended in Bohn et al. (2013).

313

314 *f. Distributed temperature and relative humidity*

315 The above-referenced standard meteorological data records have been augmented in the
316 upper Tuolumne drainage and the nearby upper Merced River drainage with widespread
317 deployment and operation of small, inexpensive temperature and humidity sensors. Daily
318 mean, minimum, and maximum temperature data from the 62 stations used in Lundquist
319 and Cayan (2007) are provided for the time period from 31 December 2000 to 1 February
320 2005. This quality-controlled dataset includes data from Onset HOBO and tidbit loggers
321 placed in evergreen trees, as well as data from area snow pillow stations, coop stations, and
322 RAWS stations, with instrument and site specifications detailed in Lundquist and Cayan
323 (2007, their Table 1 and Figure 1). While evergreen trees provide good shading from solar
324 radiation in general (Lundquist and Huggett 2008), some of the HOBO and tidbit loggers
325 were in solitary trees, which resulted in sunlight striking them at a specific angle and
326 resulted in some unrealistic maximum temperatures. Mean and minimum temperatures
327 were estimated to be accurate to within 1°C. Missing data were not patched, but an
328 analysis of how to best do so is provided in Henn et al. (2013). Raw data are available for
329 many locations at half-hourly timesteps and for a longer period of record (2001 to 2015)
330 but have not been quality controlled and thus are not detailed here.

331 Daily mean temperature and relative humidity data from 1 October 2002 to 30
332 September 2005 for the HOBO sites and snow pillow sites mentioned above are provided in
333 the Supporting Information associated with Feld et al. (2013). As with the temperature

334 data, raw data from the HOBO stations are available at half-hourly timesteps and for a
335 longer period of record (2002 to 2015) but have not been quality controlled and thus are
336 not detailed here.

337

338 **3. Discussion**

339 *a. Example scientific applications of the dataset*

340 The long timeseries and multiple nested basins lend themselves to answer many scientific
341 questions. In addition to providing insight into summer thunderstorms (e.g., Lundquist et
342 al. 2009) or diurnal cycles (e.g., Lundquist et al. 2005), which rely less on precise
343 magnitudes, the rating curves developed here allow examination of how water masses
344 move through different sections of the watershed at different times of year and during
345 different types of water years. For example, Fig. 2 illustrates half-hourly (a,d) and daily
346 average (b,e) streamflow for a wet year (2010) and a dry year (2014) for the Tuolumne
347 River at Highway 120 and the two upstream river forks that contribute to it: the Lyell Fork
348 at Twin Bridges (which drains about 60% of the area upstream, all granodiorite) and the
349 Dana Fork (which drains about 40% of the area upstream, including more metamorphic
350 and sedimentary rocks). Also shown is discharge from the Lyell Fork of the Tuolumne
351 below Maclure Creek, which isolates just the headwaters of the Lyell Fork, draining both
352 the Lyell and Maclure Glaciers and making up only 8% of the area contributing to the
353 Tuolumne at Highway 120. In 2010 there were issues with ice jams in the early season,
354 where the estimated discharge at the Lyell Twin Bridges site is higher than the estimated
355 discharge at Tuolumne 120 just downstream. These high values are likely due to ice
356 formations blocking water flow and causing local flooding. In both years, the early spring

357 flows originate mainly from the Lyell Fork (with more than 60% of flows at Tuolumne 120
358 originating from the Lyell Fork). By the time of peak runoff, 40% or more of discharge
359 originates from the Dana Fork, so that it is now contributing proportional to its area, if not
360 more so. As flows decline, the relative contribution of discharge from the Dana Fork
361 decreases, while the contribution from the Lyell Fork, particularly that originating from the
362 glaciers above Lyell below Maclure, increases. This general pattern occurs every year.
363 However, the timing of this trade-off, when Lyell below Maclure contributes more water
364 than the Dana Fork, despite its smaller area, depends on the water year. In 2010 the switch
365 occurred in mid-July (Fig. 2c), while in 2014, it occurred in mid-June (Fig. 2f). Summer
366 thunderstorms temporarily decrease the relative importance of the glacier-fed Lyell below
367 Maclure (Fig. 2 d,e,f). Also apparent are the times when contributions from the upstream
368 sub-basins exceed 100% of flow at Tuolumne 120. This may be due to incorrect estimates
369 for one or more of the rating curves (these differences fall within the 95%-uncertainty
370 bounds), or may be due to streamflow infiltrating in the meadows and restoring local
371 groundwater reserves (e.g., Loheide and Lundquist 2009; Loheide et al. 2009).

372

373 **b. Lessons learned from fieldwork: balancing trade-offs when installing in a**
374 **wilderness environment**

375 Lessons learned from the Yosemite Hydroclimate Network may be useful to inform
376 installations of similar hydroclimate networks in other wilderness locations. Ideally,
377 individual installations must be robust and inexpensive, be easy to construct and install in
378 remote regions, and need infrequent site visits. When putting a streamgauge into
379 wilderness or other protected area where installation impacts such as visibility must be

380 considered, one should consider 1) the time period of interest for monitoring (longer-term
381 requires a more robust installation), 2) accessibility and feasibility of measuring high flows,
382 3) potential ice-jamming impacts (south-facing bedrock lined channels are more robust
383 than meadow locations), 4) vented vs. unvented pressure transducers and impacts to data
384 quality/resolution (see Table 2), and 5) stability of the installation (see Table 2). Reference
385 elevations, such as benchmarks, staff gages, or tapedown measurements are also critical to
386 detect and correct for instrument movement or drift.

387

388 **4. Conclusions: Uniqueness and Application**

389 Spatially-distributed measurements are needed to understand how variations in slope,
390 aspect, elevation, soil type, vegetation, etc. influence surface processes, and these are
391 critically important in areas of high elevations and complex terrain, such as those
392 monitored with this dataset. For example, land surface climatic feedbacks and the
393 magnitude and timing of snowmelt runoff depend critically on the spatial heterogeneity of
394 snow depth and melt rates [Anderton et al., 2002; Blöschl and Sivapalan, 1995; Giorgi and
395 Avissar, 1997; Liston, 1999; Luce et al., 1998]. Current hydrologic models often get
396 approximately the right answers for the wrong reasons, and model improvements can only
397 come about through detailed checks against carefully distributed observations [Kampf and
398 Burges, 2007; Seyfried and Wilcox, 1995]. In many cases, hydrologists still struggle to
399 determine the dominant processes at different spatial scales, and even qualitative
400 observations of spatial patterns can prove invaluable in analyses [Blöschl, 2001].

401 The Tuolumne watershed has been the focus in situ distributed hydrological and
402 meteorological measurements for over 10 years, which provides a useful dataset to explore
403 distributed modeling and process representations at multiple scales.

404

405 **5. Acknowledgments**

406 The installation, maintenance, and quality-control of these sites and data has involved the
407 work of many dedicated individuals. In addition to the co-authors we thank Brian Huggett,
408 Larry Riddle, Heidi Roop, Josh Baccei, Julia Dettinger, Fred Lott, Andrey Shcherbina, Steve
409 Loheide, Chris Lowrey, Douglas Alden, Edwin Sumargo, Reuben Demirdjian and many
410 more. Funding for data processing, and hence this publication, came from the National
411 Science Foundation, CBET-0729830, and NASA Grant-NNX15AB29G. All data are currently
412 available here, <http://depts.washington.edu/mtnhydr/data/yosemite.shtml>, and at
413 CUAHSI (<http://data.cuahsi.org>), and are permanently housed in the University of
414 Washington Research Works Archive at <http://hdl.handle.net/1773/35957>. The solar
415 radiation data timeseries were quality controlled using the code provided here,
416 <https://github.com/Mountain-Hydrology-Research-Group/moq>, and the shortwave
417 interpolation algorithm is available here, <https://github.com/klapo/shin>. We thank
418 Jerome Le Coz for help setting up BaRatin and applying it to our sites. The code for BaRatin
419 can be obtained by contacting the Jerome Le Coz, as detailed in Le Coz et al. (2014).

420

421 6. References

- 422 Anderton, S.P., S. M. White, and B. Alvera (2002), Micro-scale spatial variability and the
423 timing of snow melt runoff in a high mountain catchment, *J. Hydrol.*, 268, 158-176.
- 424 Bair, E. H., K. Rittger, J. Dozier, and R. E. Davis (2016), Validating snow water equivalent
425 reconstruction using Airborne Snow Observatory measurements in the Sierra Nevada,
426 *Water Resour. Res.*, in review.
- 427 Bales, R., Molotch, N., Painter, T., Dettinger, M., Rice, R., and Dozier, J. (2006), Mountain
428 hydrology of the western US: *Water Resources Research*, 42, W08432,
429 doi:10.1029/2005WR004387.
- 430 Basagic, H. J., & Fountain, A. G. (2011), Quantifying 20th century glacier change in the Sierra
431 Nevada, California. *Arctic, Antarctic, and Alpine Research*, 43(3), 317-330.
- 432 Birgand, F., G. Lellouche, and T. W. Appelboom (2013), Measuring flow in non-ideal
433 conditions for short-term projects: Uncertainties associated with the use of stage-
434 discharge rating curves, *J. Hydrol.*, 503, 186–195, doi:[10.1016/j.jhydrol.2013.09.007](https://doi.org/10.1016/j.jhydrol.2013.09.007).
- 435 Blöschl, G. (2001), Scaling in Hydrology. *Hydrol. Process.*, 15, 709-711.
- 436 Blöschl, G. and M. Sivapalan (1995), Scale issues in hydrological modeling: a review. *Hydrol.*
437 *Proc.*, 9, 251-290.
- 438 Bohn, T. J., B. Livneh, J. W. Oyler, S. W. Running, B. Nijssen, and D. P. Lettenmaier (2013), *Ag.*
439 *and Forest Met.*, 176, 38-49. doi: <http://dx.doi.org/10.1016/j.agrformet.2013.03.003>
- 440 Coxon, G., J. Freer, I. K. Westerberg, T. Wagener, R. Woods, and P. J. Smith (2015), A novel
441 framework for discharge uncertainty quantification applied to 500 UK gauging stations,
442 *Water Resour. Res.*, 51, doi:10.1002/ 2014WR016532.

- 443 Cristea, N. C., Lundquist, J. D., Loheide, S. P., Lowry, C. S. and Moore, C. E. (2014), Modelling
444 how vegetation cover affects climate change impacts on streamflow timing and
445 magnitude in the snowmelt-dominated upper Tuolumne Basin, Sierra Nevada. *Hydrol.*
446 *Process.*, 28: 3896ñ3918. doi: 10.1002/hyp.9909
- 447 Daly, C., et al. (2008), Physiographically sensitive mapping of climatological temperature
448 and precipitation across the conterminous United States. *Int. J. Climatol.*, 28, 2031-2064,
449 doi: 10.1002/joc.1688.
- 450 Deardorff, J.W. (1978), Efficient prediction of ground surface temperature and mois-ture,
451 with an inclusion of a layer of vegetation. *J. Geophys. Res.* 83 (N64), 1889-1903,
452 <http://dx.doi.org/10.1029/JC083iC04p01889>.
- 453 Feld, S., N. C. Cristea, J. D. Lundquist (2013), Representing atmospheric moisture content
454 along mountain slopes: Examination using distributed sensors in the Sierra Nevada,
455 California, *Water Resources Research*, 49, 4424-4441, doi: 10.1002/wrcr.20318.
- 456 Freeman, L. A., M. C. Carpenter, D. O. Rosenberry, J. P. Rousseau, R. Unger, and J. S. McLean
457 (2004), Use of Submersible Pressure Transducers in Water-Resources Investigations.
458 Chapter A of Book 8, Instrumentation, Section A, Instruments for Measurement of Water
459 Level, Techniques of Water-Resources Investigations 8-A3. pp 65. [Available at:
460 <http://pubs.usgs.gov/twri/twri8a3/>]
- 461 Giorgi, F. and R. Avissar (1997), Representation of heterogeneity effects in Earth system
462 modeling: experience from land surface modeling, *Reviews of Geophysics*, 35, 413-438.
- 463 Hartsough, P.C., and Meadows, M.W. (2012), Critical Zone Observatory: Snowline Processes
464 in the Southern Sierra Nevada. *Mountain Research Initiative Newsletter no. 7, November*
465 *2012.*

- 466 Hinkelmann, L., K. Lapo, N. Cristea, and J. Lundquist (2015), Using CERES SYN Surface
467 Irradiance Data as Forcing for Snowmelt Simulation in Complex Terrain. *J.*
468 *Hydrometeorology*, 16, 2133-2152 doi:<http://dx.doi.org/10.1175/JHM-D-14-0179.1>.
- 469 Henn, B., M. P. Clark, D. Kavetski, and J. D. Lundquist (2015), Estimating mountain basin-
470 mean precipitation from streamflow using Bayesian inference. *Water Resources*
471 *Research*, 51, 8012–8033, doi: 10.1002/2014WR016736.
- 472 Henn, B., M. S. Raleigh, A. Fisher, and J. D. Lundquist (2013), A comparison of methods of
473 filling gaps in near-surface air temperature data, *Journal of Hydrometeorology*, 14, 929–
474 945. doi: <http://dx.doi.org/10.1175/JHM-D-12-027.1>
- 475 Huber, N. K. (1987), *The Geologic Story of Yosemite National Park*, U.S. Geol. Surv. Bull.,
476 1595, 64 pp.
- 477 Hudson, R. and J. Fraser (2005), Introduction to salt dilution gauging for streamflow
478 measurement part IV: The mass balance (or dry injection) method. *Streamline*
479 *Watershed Management Bulletin* 9(1): 6-12.
- 480 Hunsaker, C.T., Whitaker, T.W., and Bales, R.C. (2012), Snowmelt Runoff and Water Yield
481 Along Elevation and Temperature Gradients in California's Southern Sierra Nevada .
482 *Journal of the American Water Resources Association*, 2012. 1-12: p. 667-678.. DOI:
483 [10.1111/j.1752-1688.2012.00641.x](https://doi.org/10.1111/j.1752-1688.2012.00641.x)
- 484 Kampf, S.K. and S.J. Burges (2007), A framework for classifying and comparing distributed
485 hillslope and catchment hydrologic models. *Water Resources Research*. 43, W05423,
486 doi:10.1029/2006WR005370.
- 487 Landry, C. C., K. A. Buck, M. S. Raleigh, and M. P. Clark (2014), Mountain system monitoring
488 at Senator Beck basin, San Juan Mountains, Colorado: A new integrative data source to

- 489 develop and evaluate models of snow and hydrologic processes. *Water Resour. Res.*, 50,
490 1773–1788, doi:10.1002/2013WR013711.
- 491 Lapo, K. E. , L. M. Hinkelmann, C. C. Landry, A. K. Massmann, and J. D. Lundquist (2015), A
492 simple algorithm for identifying periods of snow accumulation on a radiometer. *Water
493 Resources Research*, 51, 7820-7828 doi: 10.1002/2015WR017590.
- 494 LeCoz, J., B. Renard, L. Bonnifait, F. Branger, and R. Le Bourcicaud (2014), Combining
495 hydraulic knowledge and uncertain gaugings in the estimation of hyrometric rating
496 curves: A Bayesian approach, *J. Hydrol.*, 509, 573-587. doi:
497 <http://dx.doi.org/10.1016/j.jhydrol.2013.11.016>
- 498 Liston, G. E. (1999), Interrelationships among snow distribution, snowmelt, and snow
499 cover depletion, implications for atmospheric, hydrologic and ecologic modeling, *J. Appl.
500 Meteorol.*, 38, 1474–1487.
- 501 Loheide, S. P. II, and J. D. Lundquist (2009), Snowmelt-induced diel fluxes through the
502 hyporheic zone. *Water Resour. Res.*, 45, W07404, doi:10.1029/2008WR007329.
- 503 Loheide, S. P. II, R. S. Deitchman, D. J. Cooper, E. C. Wolf, C. T. Hammersmark, and J. D.
504 Lundquist (2009), Hydroecology of impacted wet meadows in the Sierra Nevada and
505 Cascade Ranges, CA. *Hydrogeology Journal*, 17, 229–246, doi: 10.1007/s10040-008-
506 0380-4.
- 507 Lowry, C., J. Deems, S. Loheide II, and J. D. Lundquist (2010), Linking snowmelt derived
508 recharge and groundwater flow in a high elevation meadow system, Sierra Nevada
509 Mountains, California. *Hydrological Processes*, 24, 2821-2833.

- 510 Lowry, C. S. P. Loheide, C. Moore, J. D. Lundquist (2011), Groundwater controls on
511 vegetation composition and patterning in mountain meadows, *Water Resources*
512 *Research*, 47, W00J11, doi:10.1029/2010WR010086.
- 513 Luce, C. H., D. G. Tarboton, and K. R. Cooley (1998), The influence of the spatial distribution
514 of snow on basin-averaged snowmelt, *Hydrol. Processes*, 12, 1671–1683.
- 515 Lundquist, J. D., and M. D. Dettinger (2005), How snowpack heterogeneity affects diurnal
516 streamflow timing, *Water Resour. Res.*, 41, W05007, doi:10.1029/2004WR003649.
- 517 Lundquist, J. D. and J. Roche (2009), Climate change and water supply in western national
518 parks, *Park Science*, ISSN 1090-9966.
- 519 Lundquist, J. D., D. R. Cayan, and M. D. Dettinger (2003), Meteorology and hydrology in
520 Yosemite National Park: A sensor network application, in Information Processing in
521 Sensor Networks: Second International Workshop, IPSN 2003, edited by F. Zhao and L.
522 Guibas, pp. 518– 528, Springer, New York.
- 523 Lundquist, J. D., D. R. Cayan, and M. D. Dettinger (2004), Spring onset in the Sierra Nevada:
524 When is snowmelt independent of elevation?, *J. Hydrometeorol.*, 5, 325– 340.
- 525 Lundquist, J. D., M. Dettinger, and D. Cayan (2005), Snow-fed streamflow timing at different
526 basin scales: Case study of the Tuolumne River above Hetch Hetchy, Yosemite,
527 California. *Water Resour. Res.*, 41, W07005, doi: 10.1029/2004WR003933.
- 528 Lundquist, J. D. and A. Flint (2006), Onset of snowmelt and streamflow in 2004 in the
529 Western United States: How shading may affect spring streamflow timing in a warmer
530 world. *J. Hydrometeorology*, 7, 1199-1217.

- 531 Lundquist, J. D. and D. R. Cayan (2007), Surface temperature patterns in complex terrain:
532 daily variations and long-term change in the central Sierra Nevada, California. *J. Geophys.*
533 *Res.*, 112, D11124, doi:10.1029/2006JD007561.
- 534 Lundquist, J.D., N. Pepin, and C. Rochford (2008), Automated algorithm for mapping regions
535 of cold-air pooling in complex terrain, *J. Geophys. Res.*, 113, D22107,
536 doi:10.1029/2008JD009879.
- 537 Lundquist, J. D. and B. Huggett (2008), Evergreen trees as inexpensive radiation shields for
538 temperature sensors, *Water Resources Research*, special issue on Measurement Methods,
539 44, W00D04, doi:10.1029/2008WR006979.
- 540 Lundquist, J. D., B. Huggett, H. Roop, and N. Low, (2009), Use of spatially-distributed stream
541 stage recorder to augment rain gages by identifying locations of thunderstorm
542 precipitation and distinguishing rain from snow. *Water Resources Research*, 45,
543 W00D25, doi:10.1029/2008WR006995.
- 544 Lundquist, J. D., Wayand, N. E., Massmann, A., Clark, M. P., Lott, F. and Cristea, N. C. (2015),
545 Diagnosis of insidious data disasters. *Water Resources Research*, 51(4), 2498-2514. doi:
546 10.1002/2014WR016585
- 547 Moore, C. E, S. P. Loheide, C. S. Lowry, and J. D. Lundquist (2014), Instream restoration to
548 improve the ecohydrologic function of a subalpine meadow: pre-implementation
549 modeling with HEC_RAS. *Journal of the American Water Resources Association (JAWRA)*,
550 1-17. doi: 10.1111/jawr.12155.
- 551 Moore, R.D. (2004a). Introduction to Salt Dilution Gauging for Streamflow Measurement:
552 Part 1. *Streamline Watershed Management Bulletin* 7(4): 20-23

- 553 Moore, R.D. (2004b). Introduction to salt dilution gauging for streamflow measurement.
- 554 Part 2: Constant-rate injection. *Streamline Watershed Management Bulletin* 8(1): 11-15.
- 555 Moore, R.D. (2005), Introduction to salt dilution gauging for streamflow measurement. Part
- 556 3: Slug injection. *Streamline Watershed Management Bulletin* 8(2): 1-6.
- 557 Muir, J. (1911), *My First Summer in the Sierra*, Dunwoody, GA: Norman S. Berg, Publisher.
- 558 Natural Resources Conservation Service (2006), Soil Survey Geographic (SSURGO)
- 559 database for Yosemite National Park, California, ca790, U.S. Dep. of Agric., Washington,
- 560 D. C. (Available at <http://SoilDataMart.nrcs.usda.gov>.)
- 561 Oberg, K., and D. S. Mueller (2007), Validation of streamflow measurements made with
- 562 acoustic Doppler current profilers. *J. Hydraulic Eng. ASCE*, 133, 1421-1432.
- 563 O'Neill, E. S. (1984), *Meadow in the Sky: A History of Yosemite's Tuolumne Meadows Region*,
- 564 Albicaulis Press, Groveland, California, 179 p.
- 565 Painter, T. H. et al. (2015), The Airborne Snow Observatory: scanning lidar and imaging
- 566 spectrometer fusion for mapping snow water equivalent and snow albedo, submitted to
- 567 *Remote Sens. Environ.*
- 568 Prata, A.J., (1996), A new long-wave formula for estimating downward clear-sky radiation
- 569 at the surface. *Q. J. R. Meteor. Soc.* 122 (533), 1127–1151,
- 570 <http://dx.doi.org/10.1002/qj.49712253306>.
- 571 Raleigh, M. S., Rittger, K., Moore, C. E., Henn, B., Lutz, J. A., & Lundquist, J. D. (2013). Ground-
- 572 based testing of MODIS fractional snow cover in subalpine meadows and forests of the
- 573 Sierra Nevada. *Remote Sensing of Environment*, 128, 44-57.
- 574 Rantz, S. E. et al. (1982a), Measurement and Computation of Streamflow, vol. 1,
- 575 Measurement of Stage and Discharge, U.S. Geol. Surv. Water Supply Pap., 2175, 284 pp.

- 576 Rantz, S.E., and others, (1982b), Measurement and computation of streamflow: Volume 2,
577 Computation of discharge: U.S. Geological Survey Water-Supply Paper 2175, v. 2, p. 285-
578 631.
- 579 Reba, M. L., D. Marks, M. Seyfried, A. Winstral, M. Kumar, and G. Flerchinger (2011), A long-
580 term data set for hydrologic modeling in a snow-dominated mountain catchment. *Water*
581 *Resources Res.*, 47, W07702, doi:10.1029/2010WR010030.
- 582 Rice, R., Bales, R. C., Painter, T. H., & Dozier, J. (2011), Snow water equivalent along
583 elevation gradients in the Merced and Tuolumne River basins of the Sierra
584 Nevada. *Water Resources Research*, 47(8).
- 585 Rittger, K., T. H. Painter, and J. Dozier, (2013), Assessment of methods for mapping snow
586 cover from MODIS, *Advances in Water Resources*, 51, 367-380,
587 <http://dx.doi.org/10.1016/j.advwatres.2012.03.002>.
- 588 Rittger, K., A. Kahl, and J. Dozier (2011), Topographic distribution of snow water equivalent
589 in the Sierra Nevada, Proc. Western Snow Conf., 79, 37-46,
590 <http://www.westernsnowconference.org/node/781>.
- 591 Seyfried, M. S., and B. P. Wilcox (1995), Scale and the nature of spatial variability: Field
592 examples having implications for hydrologic modeling, *Water Resour. Res.*, 31, 173–184.
- 593

594

595

596

597

598

599

600

7. Tables

Table 1: List of stream sites, locations and data availability, all geographic coordinates use NAD 83 datum. Order matches supplemental material, from upstream to downstream. *Some sites are also locations of USGS water quality monitoring, and their USGS site ID numbers are referenced.

** Real-time values available at: <http://cdec.water.ca.gov/cgi-progs/queryF?s=TUM>

Site Code	USGS Site ID*	Site Name	Latitude	Longitude	Basin Area	Elevation	Water Years with Data (X=data available)															Type of installation
			Degrees	Degrees	km ²	meters	0 2	0 3	0 4	0 5	0 6	0 7	0 8	0 9	1 0	1 1	1 2	1 3	1 4	1 5		
HB270	37464011 9154100	Lyell below Maclare	37.777	-119.261	15	2940			X	X	X		X	X	X	X	X	X	X	X	Solinst, Stilling tube	
																					X	Vented Transducer
H03a (NP269)	37521011 9195000	Lyell Fork, upstream	37.869	-119.331	109	2640				X	X	X	X	X	X	X	X	X	X	X	Solinst, Stilling tube; Vented transducer installed 7/16/2015	
H03b		Lyell Fork, downstream	37.869	-119.331	109	2640	X	X	X	X	X	X	X		X	X					Solinst, anchor	
H02a (NP188)	37523311 9200401	Dana Fork, lodge	37.876	-119.333	74	2650	X	X	X	X	X										Solinst, anchor	
H02b		Dana Fork, Bug Camp	37.877	-119.338	75	2640				X	X	X	X	X	X	X	X	X	X	X	Solinst, Stilling tube; Vented transducer (6/12/2015-present)	
NP238	37523411 9211400	Tuolumne 120	37.876	-119.355	186	2600	X	X	X	X										Solinst, anchor		
										X	X			X	X	X	X	X	X	X	Solinst, Stilling tube	
																				X	X	Vented

																				installed 10/2012.**
H07		Delaney Creek, meadow	37.883	-119.381	16	2600						X	X	X	X	X	X	X	X	Solinst, Stilling tube
H01a		Budd Creek upstream	37.873	-119.382	7	2600					X	X	X	X	X		X	X	X	Solinst, Stilling tube
H01b		Budd Creek downstream	37.874	-119.382			X	X	X	X	X			X		X	X	X	X	Solinst, anchor
H99		Hetch Hetchy Reservoir	37.9708	-119.788 3	1181	1162	X	X	X	X	X	X	X	X	X	X	X	X	X	See text
AF01		Dana Snow Pillow	37.896	-119.257	NA	3000	X	X	X	X	X	X	X	X	X	X	X	X	X	See text

601

602 Table 2. Stream Sensor Instrument Installations: types and accuracy

603 *Note that the Levelogger Gold reports water level equivalent above the datalogger's pressure zero point of 950 cm (the Edge
 604 models do not have such an offset.) ¹Druck was used at Delaney Cr above PCT from 2012-2015; ²Campbell Scientific CS450
 605 was used at Lyell below Maclare 2012-present; Tuolumne at 120 2012-present; Dana at Bug Camp 2014-present; Lyell above
 606 Twin Bridges 2015-present.

Installation Type	Anchored Solinst*	Solinst in Stilling Tube	Vented Pressure Transducer	Barometric Pressure
Description	Instrument in a PVC pipe inside a concrete anchor, which is cabled to a tree, bridge, or culvert.	Instrument in PVC pipe inserted in vertical pipe attached to the streambed and bank with rebar; with cord for downloading instrument.	Same as stilling tube but with data cord connected to a data logger box (typically hidden in a tree) and another cord open to the atmosphere.	Instrument in a building or in a tree or in a dry groundwater well
Instrument Used	Solinst Levelogger	Solinst Levelogger	Druck ¹ Or Campbell Scientific CS450 PT ²	Solinst Barologger
Instrument Specs/Accuracy	Levelogger Model 3001: 0.1°C temp accuracy, ±0.5 cm pressure/depth accuracy; temperature compensated over the range of -10 to 40°C; drift of 0.1% of the full range (±0.5 cm for a 5 m model, used here).	Levelogger Edge and Gold: Temp accuracy ± 0.05°C Pressure ± 0.05% of FS (for 5 m model, this would be ±0.25 cm); Manufacturer states clock accurate to 1 minute per year, but 20 minutes of drift per year was typically observed in practice	Druck: 0-5 PSI Range, 0.25% accuracy; CS450: 0-7.25 PSI Range, 0.1% accuracy;	Edge: ± 0.05 kPa, with temperature compensation, temperature accuracy ± 0.05°C Gold: 0.01 cm and ± 0.05°C (also has temp compensation); Model 3001 same as 5 m Levelogger.
Processing steps	1) subtract off	1, 3, and 4	3 and 4	3, and 5) adjust

required	atmospheric pressure; 2) correct for offsets in instrument location; 3) check for instrument drift; 4) develop rating curve			for temperature dependencies
Total error estimates in stage (Note that these are worst case scenarios – errors for most sites are believed to be less.)	Up to \pm 3 to 4 cm, with \pm 2 cm due to summed instrument accuracy and drift for both stream and barometric instruments; and \pm 1 to 2 cm more due to uncertainty in instrument location	Up to \pm 2 cm due to summed instrument accuracy and potential drift for both stream and barometric instruments	Up to \pm 0.5 cm due to summed instrument accuracy and potential drift	Up to \pm 1 cm due to summed instrument accuracy and potential drift
Error propagation into estimated discharge (using Lyell Fork above Twin Bridges at 0.7 m, typical summer flow, as an example)	\pm 0.92 $m^3 s^{-1}$ to \pm 1.24 $m^3 s^{-1}$ (14-19%)	\pm 0.61 $m^3 s^{-1}$ (9%)	\pm 0.15 $m^3 s^{-1}$ (2%)	\pm 0.30 $m^3 s^{-1}$ (5%)
Pros	Easy installation, lowest visible impact	Low visible impact; stable location and datum	Stable location and datum; lowest processing time required (saves ~8 hours of desk work per year); can reference instrument stage to field datum at each visit	
Cons	Instrument location moves through time; Most processing time	Error increases with atmospheric adjustment; hard to reference	More work required to reduce visible impact (e.g., hiding conduit and annual	

	required (~8 hours of desk work per year per site by trained person + ~2 weeks additional time training for new person);	instrument reading to field datum while in the field	battery swap from a hidden battery enclosure); higher instrument cost	
--	--	--	---	--

607

608

609

610

611

612
613
614

8. Figures

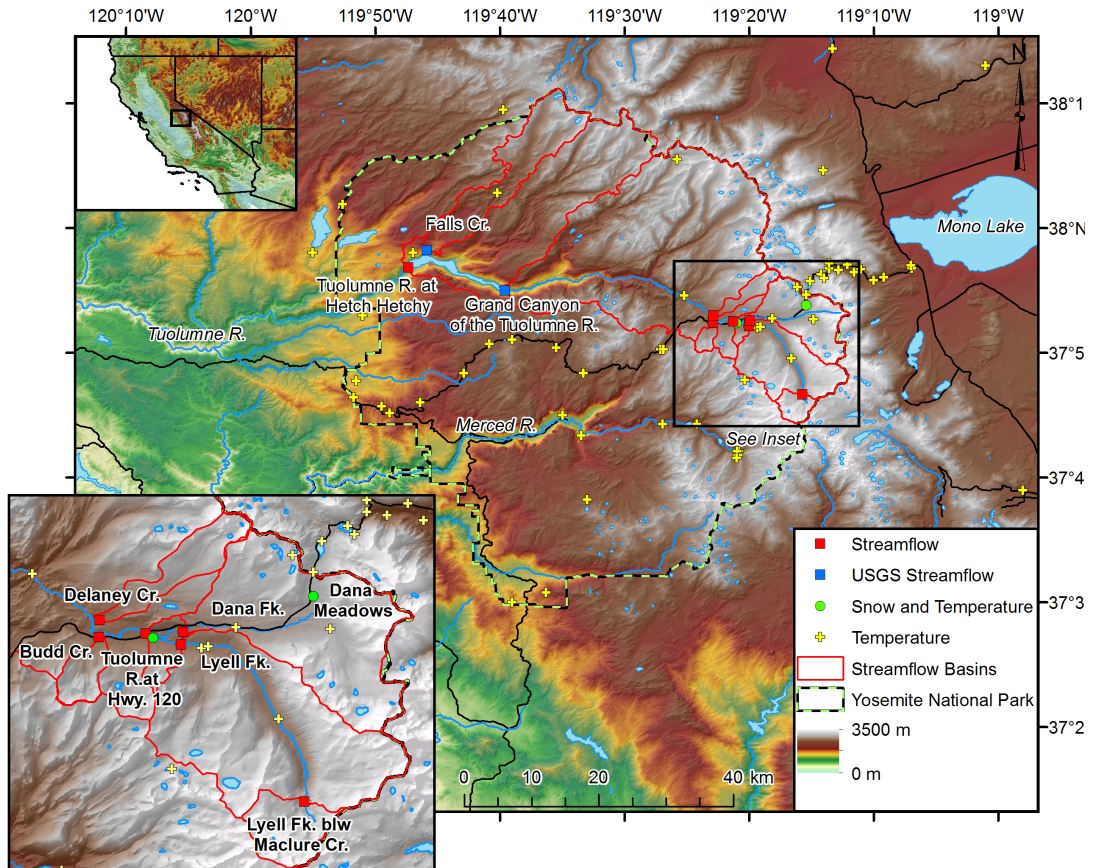
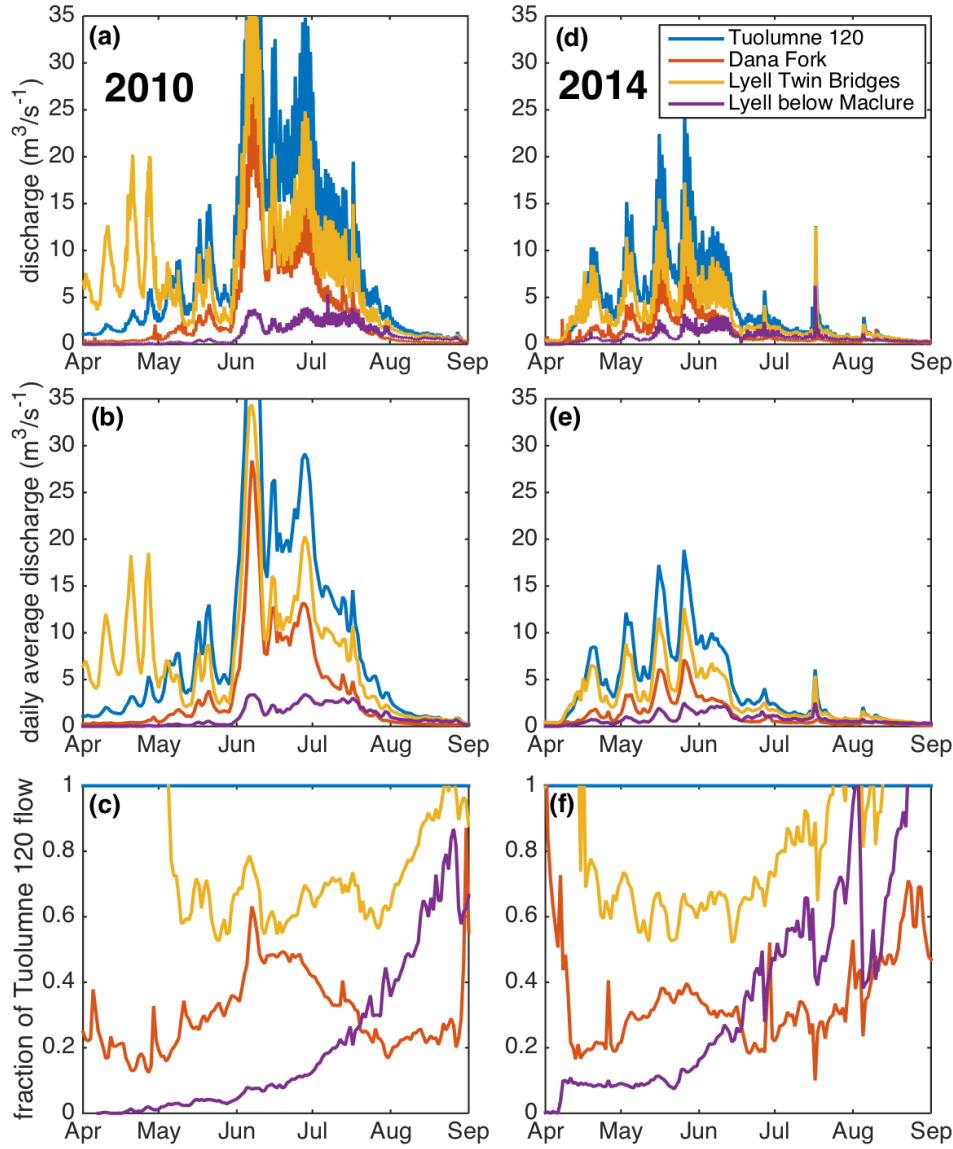
615
616
617
618
619
620
621
622
623
624
625

Fig. 1. Map of all data sites included in this paper. The yellow crosses are temperature sensor locations. The Falls Creek and Grand Canyon of the Tuolumne are USGS gauge locations, and the red squares are streamflow sites included in the archive. The green dots were used to create the meteorological forcing dataset (with precipitation only taken from the Tuolumne site and all other values taken from the Dana Meadows site).



626

627 Figure 2. Illustration of dynamic discharge relationships for (a,d) half-hourly flows
 628 and (b,e) daily average flows of the Dana Fork, Lyell Fork below Maclure, Lyell Fork
 629 at Twin Bridges and Tuolumne at 120. (c,f) Flows at the three higher gages as a
 630 fraction of daily flows at Tuolumne 120. Plots show these four subbasins in a cool-
 631 wet year (2010, a,b,c) and a warm-dry year (2014, d,e,f). By area, the Dana Fork and
 632 Lyell Fork at Twin Bridges make up about 40% and 60% of the Tuolumne at 120
 633 drainage. The Lyell below Maclure monitors just the headwaters of the Lyell Fork,
 634 and makes up about 8% of the area contributing to Tuolumne at 120. See text for
 635 discussion.